FCC-ee RADIATION ENVIRONMENT AND SHIELDING

B. Humann*, A. Lechner, M. Ady, T.G. Banks, J. Bauche, D. Bozzato, J.P. Burnet, M. Calviani, F. Carra, R. Cowan, A. Frasca[1], R. Garcia Alia, C. Garion, D. Hajdu, K. Hanke, M. Jebramcik, G. Lavezzari, G. Lerner, I. Martin Melero, M. Morrone, D. Najdrowski, A. Perillo Marcone, A. Piccini, A. Romero Francia, K. Taylor, M. Timmins, M. Widorski, CERN, Geneva, Switzerland
F. Valchkova-Georgieva, CEGELEC SA, Carouge, Switzerland
[1]also at University of Liverpool, Liverpool, UK

Abstract

In a high-energy lepton collider such as the Future Circular Collider (FCC-ee) at CERN, phenomena like synchrotron radiation (SR) create a challenging radiation environment for accelerator components and equipment including cables and electronics. This paper examines the radiation load in the collider arcs at the highest beam energies ($\mathrm{t\bar{t}}$) for two different optics schemes. Recent developments in the design of photon stoppers and dedicated radiation shielding are presented, highlighting progress towards a more realistic configuration while maintaining acceptable annual ionizing dose levels. The absorbed power in accelerator components and the surrounding tunnel environment is evaluated for various operation modes to ensure compliance with the thermal load limits of the ventilation system. Furthermore, neutron spectra due to photo-neutron production are quantified for the electronics bunkers located below the beamline, and the feasibility of employing radiation-tolerant, commercial-off-the-shelf electronics in these areas is assessed. Finally, a first evaluation of the radiation field in the alcoves, housing radiation-sensitive equipment, is presented.

INTRODUCTION

In an electron-positron collider like the Future Circular Collider (FCC-ee) at CERN, synchrotron radiation (SR) is one of the main contributors to the radiation load on the accelerator equipment and environment. FCC-ee will be operated at four energies, ranging from 45.6 GeV (Z pole) to 182.5 GeV ($\mathrm{t\bar{t}}$) [1]. The radiation field is characterised by the critical energy, $E_C \propto E^3$, which divides the photon spectrum into two equal-power halves. A higher critical energy implies a harder photon spectrum, leading to more penetrating secondary particles and an increased photo-neutron contribution. Two optics schemes are compared in this study focusing on the $\mathrm{t\bar{t}}$ operation mode, which produces the hardest SR spectrum. The GHC (global hybrid correction) optics [2] has been the baseline optics in the past years, while the LCC (local chromaticity correction) optics [3] is a newer design. The LCC lattice exhibits a higher dipole filling factor, which in turn yields a larger bending radius (ρ_{LCC} =10.91 km, ρ_{GHC} =10.04 km). This results in a mover favourable radiation environment, owing to the $1/\rho$ dependence of the SR energy loss and the critical photon energy. The corresponding values are listed in Table 1 for the Z pole and the $\mathrm{t\bar{t}}$ operation modes. For GHC, the SR power is assumed by design to be 50 MW/beam for all operation modes, corresponding to 11.3 MW for one arc (8.96 km) or 630 W/m/beam. Assuming the same beam current for LCC, the larger filling factor in LCC reduces the emitted power by 7% to 585 W/m/beam.

Table 1: Energy loss per turn ($\frac{\Delta E}{\mathrm{turn}}$), the critical energy ($E_C$), and the beam current (I_{Beam}) for the Z and $\mathrm{t\bar{t}}$ working points in both optics schemes.

	Z		tt	
	GHC	**LCC**	**GHC**	**LCC**
$\frac{\Delta E}{\mathrm{turn}}$	0.039 GeV	0.035 GeV	10.01 GeV	8.98 GeV
E_C	0.022 MeV	0.019 MeV	1.37 MeV	1.24 MeV
I_{Beam}	1285 mA		5 mA	

The radiation load is assessed with FLUKA Monte Carlo simulation [4–7] for one FODO cell of the $\mathrm{t\bar{t}}$ operation mode (Fig. 1). This paper builds upon previous radiation transport studies and shielding design iterations presented in [8–11], which is further developed in [12]. Recent updates to the design of the localized SR absorbers (SRA), the dipole, and the surrounding lead shielding are presented, targeting a reduction of the radiation load in the tunnel. The electronics bunker design presented in [10] is revisited, showing an increase in dimensions and a relocation to below the dipoles. Finally, a first assessment of the radiation field in the alcoves, located perpendicular to the accelerator tunnel, is presented.

SHIELDING ASSEMBLY DEVELOPMENTS

The 38 cm long SRAs intercepting the SR photons are made of a copper alloy (CuCrZr) and are placed in the winglets of the vacuum chamber (see Fig. 2) [13–15]. The vertical dimension of the SRAs has been increased to span the full available height within the dipole yoke, enhancing the shielding performance. A cooling plate is foreseen at

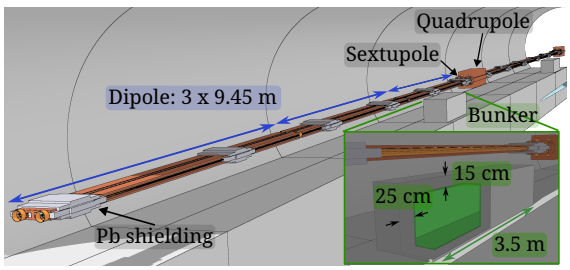

Figure 1: 63 m FODO cell (LCC) implemented in FLUKA.

* barbara.humann@cern.ch

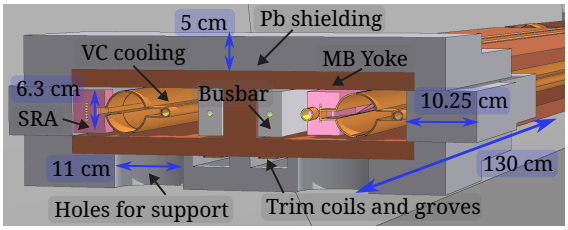

Figure 2: Cross section of the dipole assembly including the vacuum chamber (VC), the SRA, and the Pb shielding.

the interface between the dipole yoke and the lead shielding [12], which is not included in the FLUKA model, as its impact on the radiation load has been shown to be negligible. The surrounding lead shielding (760 kg per 2 SRA) has undergone significant changes compared to [10]. While the outer envelope has remained largely identical, most inserts around the winglet have been removed to allow for a simpler and cost-efficient engineering solution. A simplified insert geometry is retained only at locations where the forward component of secondary showers from the SRA would otherwise lead to insufficient shielding. Holes introduced in the bottom of the shielding for the magnet supports locally reduce the shielding material and are consequently relevant for the radiation load in the tunnel. Finally, the shielding material has been changed from an antimony-lead alloy to pure lead (ρ_{Pb} =11.34 g/cm^3, 99.9% purity), as mechanical stability can be met and is the more cost-efficient option. Both, the SRA and the shielding design, are identical for both optics schemes.

In the FODO cell of the LCC optics (63 m), the dipoles consist of three magnets of 9.45 m each, with four SRAs and two shielding structures. The longest gap between two SRAs of 5.14 m occurs around the short straight section (SSS). This regular layout offers a significant advantage over the GHC optics, where each dipole was split into a longer magnet of 12 m (3 SRAs/beam) and one shorter one of 7 m, 9 m, or 10 m (2 SRAs/beam), and the longest gap between two SRAs reaches 7.85 m around the SSS.

RADIATION LOAD IN THE FODO CELL

SR photons impacting the SRAs deposit energy and produce showers of secondaries, which reach other accelerator components and the tunnel environment. At the Z pole, the SRAs absorb the largest fraction of SR power, around 96%. At $\mathrm{t\bar{t}}$, this fraction drops to 81% as SR photons undergo Compton scattering on the SRAs. These values are higher compared to the past studies [10] due to the increase SRA volume. Table 2 lists the absorbed power on the SRAs for both optics schemes. Due to the higher filling factor, the average power is around 7% lower for LCC at both working points. The more regular longitudinal SRA placement and shorter SSS in LCC result in a reduced spread of absorbed power across SRAs, simplifying cooling requirements. In contrast, the GHC optics would require more sophisticated cooling and engineering solutions, as the maximum power

Table 2: Power deposition by SR in the SRAs for both optics schemes for Z pole and $\mathrm{t\bar{t}}$ operation.

		GHC	LCC
Z	Range	2.6 kW - 4.7 kW	2.5 kW - 3.3 kW
	Average	3.3 kW	3.1 kW
$\mathrm{t\bar{t}}$	Range	1.8 kW - 3.9 kW	2.0 kW - 2.7 kW
	Average	2.7 kW	2.5 kW

load at the Z pole exceeds what the current design can handle reliably [16].

One of the key considerations in the shielding design is the SR-induced heat load within the tunnel environment, which must be removed through the ventilation system. The majority of heat deposition in the tunnel originates from heat transfer between machine components and the surrounding air, whereas the contribution from secondary particles escaping the SRAs and shielding is negligible ($\mathrm{t\bar{t}}$: 0.05%, Z pole: <0.01%). Consequently, effective water-cooling of various machine components, including the SRAs, bus-bars, shielding, and dipole yokes, is essential.

For the SRAs and the vacuum chamber (VC), a cooling efficiency of 99.85% is assumed. A cooling plate attached to the yoke dissipates the heat from the lead shielding and the yoke, with an efficiency strongly dependent on the tunnel air temperature, ranging from 18.5% at 16 °C to 86.7% at 32 °C. For the GHC optics, the total heat dissipated into the tunnel air reaches 1.3 MW per arc at 16 °C. At 32 °C, this reduces to 221 kW, as the cooling plate efficiency increases strongly with tunnel air temperature. Currently, tunnel operation in the range of 28 °C to 32 °C is foreseen, which helps maintain a stable thermal environment around the collider magnets [17].

Long term radiation effects mainly caused by the cumulative ionizing dose, impact accelerator equipment like cables or optical fibres, leading to material degradation and reduced equipment lifetime. With the current shielding design in the LCC optics, annual dose levels at the cable tray locations on the tunnel wall, 2 m above the beamline, are around 10 kGy for $\mathrm{t\bar{t}}$ (see Fig. 3), corresponding to less than 100 kGy over the full FCC-ee operational lifetime, permitting the use of cost-efficient, general-purpose cables [18]. The holes for the magnet support in the shielding cause dose levels below the shielding units of <300 kGy, necessitating radiation-hard equipment in these locations. Given that each FCC-ee arc contains more than 1600 shielding units, reducing this dose level would have a significant impact on equipment costs. Reducing the size or filling the holes with material could mitigate this issue.

ELECTRONICS BUNKERS

While the SRA and lead shielding design significantly reduce the radiation levels in the tunnel, the remaining radiation field still exceeds the tolerance of radiation sensitive electronics. Excessive dose levels reduce equipment lifetime, and neutron-induced effects such as Single Event

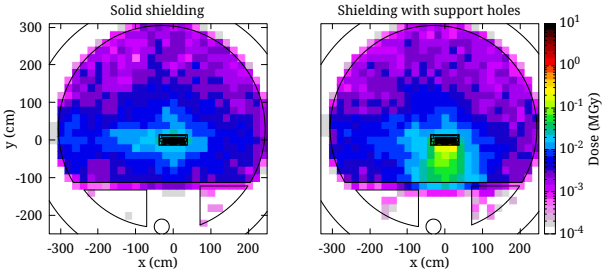

Figure 3: Annual (185 days, 75% efficiency) dose levels for the LCC optics at a shielding location for a solid shielding and a shielding with holes for supports.

Effects (SEE) can cause machine downtime. Electronics for systems like beam loss monitors, beam position monitors, and vacuum systems must nevertheless be located close to the machine. Therefore, dedicated electronics bunkers are foreseen in the design of the FODO cell.

The electronics bunkers are located at the end of the dipoles (see Fig. 1), where sufficient space is available. A proposal to integrate the bunkers into the quadrupole girders [10] was abandoned due to space constraints. Each bunker is sized to accommodate three electronics racks, with 25 cm thick concrete walls at the front and rear and 15 cm for the remaining walls. The inner walls are lined with a 2 cm thick layer of 10% borated polyethylene to thermalize and capture neutrons, which are the main source of radiation effects in a shielded environment like the bunker.

This shielding concept is designed to provide a radiation environment compatible (up to a total of 0.5 kGy-1 kGy [10]) with the use of radiation-tolerant electronics design based on commercially-off-the-shelf (COTS) components. The bunker design is at a preliminary stage, with several technical aspects still to be addressed, including the integration of a sliding access door and the cooling and ventilation systems required for reliable electronics operation.

The feasibility of COTS components in such a bunker concept was demonstrated in [10]. Here, the neutron spectra for both optics schemes are compared. Figure 4 shows the neutron spectra at various positions in the machine for both optics. Due to the higher critical energy (see Table 1), the neutron fluence coming from the absorbers is a factor of 2 higher for GHC, as the SR spectrum is shifted towards higher energies and increasing the overlap with the Giant Dipole Resonance. The lead shielding around the absorbers attenuates the neutron fluence. Within the bunker concrete shielding, the spectra for both optics are nearly identical,

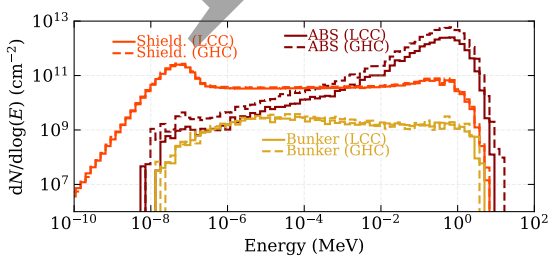

Figure 4: Annual neutron fluence next to the SRAs, in the bunker walls (shield) and in the bunker for both optics.

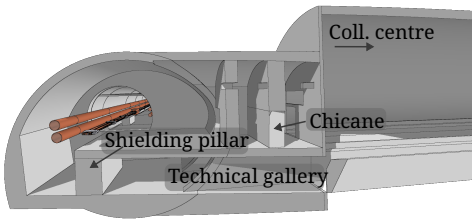

Figure 5: Integration of the alcove into the LCC FODO cell.

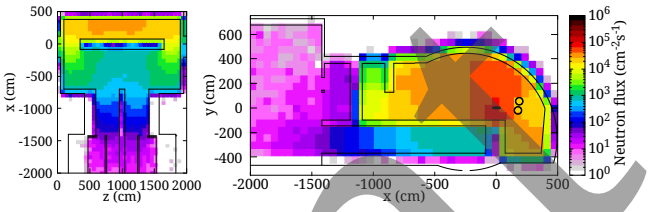

Figure 6: Neutron flux in the accelerator tunnel (LCC optics), the technical gallery and the alcove as a top view of the technical gallery and a cross section at a chicane opening.

with a thermal peak at around 0.1 eV. The concrete shielding and borated polyethylene layer reduce the neutron contribution by a further order of magnitude, with the borated polyethylene specifically acting on the low-energy neutron absorption. The resulting SEE risk in the bunker is similar for both optics schemes.

ALCOVES

A model of the alcove has recently been incorporated into the FLUKA model of the FODO cell (see Fig. 5). In each arc, 7 alcoves [16] will house equipment such as magnet power supplies and systems for vacuum, radiation protection, and beam instrumentation. The radiation environment in the alcoves should be designed to permit the use of any COTS electronics. At the accelerator level, a chicane is foreseen to reduce the neutron fluence in the alcove while allowing access. Equipment connections are routed through the technical gallery one level below. The 1.67 m thick shielding pillar reduces the neutron flux in the technical gallery by at least one order of magnitude (see Fig. 6). The remaining neutron flux in the technical gallery provides a first indication that further shielding optimisation may be required, and dedicated simulations with improved statistics are required for a conclusive radiation field assessment.

CONCLUSIONS

This paper has shown that the LCC optics scheme is preferable, owing to its more regular layout and consequently more uniform heat load distribution. With the current SRA and lead shielding design, annual dose levels of around 10 kGy at the cable tray locations are compatible with the use of general-purpose cables. The neutron contribution in the electronics bunkers is similar for both optics schemes, supporting the feasibility of radiation-tolerant COTS electronics in these areas. Improved simulations are planned to quantify the radiation environment in the alcoves and assess the viability of COTS electronics in this region.

REFERENCES

[1] A. Abada *et al.*, "FCC-ee: The Lepton Collider", *Eur. Phys. J. Spec. Top.*, vol. 228, pp. 261–623, 2019. doi:10.1140/epjst/e2019-900045-4

[2] K. Oide *et al.*, "Design of beam optics for the future circular collider e^+e^- collider rings", *Phys. Rev. Accel. Beams*, vol. 19, no. 11, p. 111005, Nov. 2016. doi:10.1103/PhysRevAccelBeams.19.111005

[3] P. Raimondi, S. M. Liuzzo, L. Farvacque, S. White, and M. Hofer, "Local chromatic correction optics for future circular collider e^+e^-", *Phys. Rev. Accel. Beams*, vol. 28, no. 2, p. 021002, Feb. 2025. doi:10.1103/PhysRevAccelBeams.28.021002

[4] FLUKA website, `https://fluka.cern`,

[5] C. Ahdida *et al.*, "New Capabilities of the FLUKA Multi-Purpose Code", *Front. Phys.*, vol. 9, 2022. doi:10.3389/fphy.2021.788253

[6] G. Battistoni *et al.*, "Overview of the FLUKA code", *Ann. Nucl. Energy*, vol. 82, pp. 10–18, 2015. doi:10.1016/j.anucene.2014.11.007

[7] G. Hugo *et al.*, "Latest FLUKA developments", *EPJ N Nucl. Sci. Technol.*, vol. 10, p. 20, 2024. doi:10.1051/epjn/2024023

[8] B. Humann, F. Cerutti, and R. Kersevan, "Synchrotron radiation impact on the FCC-ee arcs", in *Proc. IPAC'22*, Bangkok, Thailand, 2022, pp. 1675–1678. doi:10.18429/JACoW-IPAC2022-WEPOST002

[9] B. Humann *et al.*, "Challenges and mitigation measures for synchrotron radiation on the FCC-ee arcs", in *Proc. IPAC'24*, Nashville, TN, USA, 2024, pp. 292–295. doi:10.18429/JACoW-IPAC2024-MOPG04

[10] A. Lechner *et al.*, "Fcc-ee radiation environment and shielding", in *Proc. IPAC'25*, Taipei, Taiwan, pp. 482–485, Jun. 2025. doi:10.18429/JACoW-IPAC2025-MOPM068

[11] A. R. Francia *et al.*, "Mechanical design and challenges of the FCCee arc radiation shielding", in *Proc. IPAC'25*, Taipei, Taiwan, pp. 2638–2641, Nov. 2025. doi:10.18429/JACoW-IPAC2025-THPB060

[12] R. Cowan *et al.*, "Design Refinements And Prototyping Of Lead Shielding For The FCC-ee Arc Dipoles", presented at IPAC'26, Deauville, France, May 2026, paper WEP1017, this conference,

[13] R. Kersevan and C. Garion, "Conceptual design of the vacuum system for the Future Circular Collider FCC-ee main rings", in *Proc. IPAC'21*, Campinas, SP, Brazil, May 2021, pp. 2438–2440. doi:10.18429/JACoW-IPAC2021-TUPAB392

[14] R. Kersevan, "The FCC-ee vacuum system, from conceptual to prototyping", *EPJ Tech. Instrum.*, vol. 9, no. 1, p. 12, 2022. doi:10.1140/epjti/s40485-022-00087-w

[15] M. Morrone *et al.*, "Preliminary design of the FCC-ee vacuum chamber absorbers", in *Proc. IPAC'23*, Venice, Italy, May 2023, pp. 382–385. doi:10.18429/JACoW-IPAC2023-MOPA141

[16] M. Benedikt *et al.*, "Future Circular Collider Feasibility Study Report Volume 2: Accelerators, technical infrastructure and safety", CERN, Geneva, Switzerland, Geneva, Switzerland, Rep. CERN-FCC-ACC-2025-0004, 2025. doi:10.17181/CERN.EBAY.7W4X

[17] A. Coleman, Private communication, Mar. 2026,

[18] H. Garcia *et al.*, "HL-LHC Outcome of the cabling Market Survey", CERN, Geneva, Switzerland, Rep., 2022.